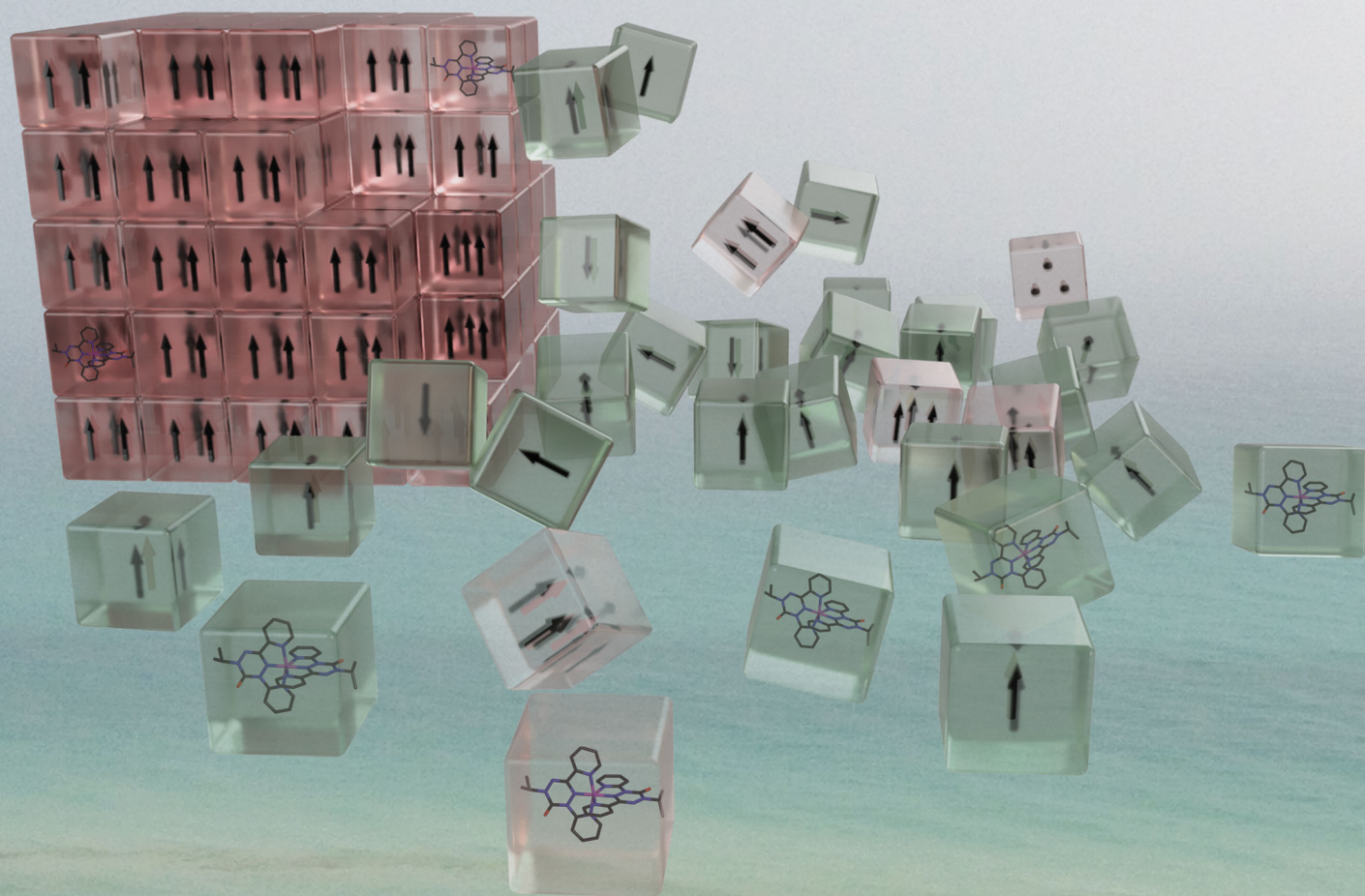


ChemComm

Chemical Communications

rsc.li/chemcomm



ISSN 1359-7345

COMMUNICATION

David J. R. Brook *et al.*
Valence tautomerism in a cobalt-verdazyl coordination
compound



Valence tautomerism in a cobalt-verdazyl coordination compound†

Cite this: *Chem. Commun.*, 2020, 56, 4400

Received 6th March 2020,
Accepted 26th March 2020

DOI: 10.1039/d0cc01770a

rsc.li/chemcomm

Connor Fleming,^a Dorothy Chung,^a Servando Ponce,^a David J. R. Brook,^{ib} *^a
Jeffrey DaRos,^a Raja Das,^b Andrew Ozarowski^{ib} ^c and Sebastian A. Stoian^{ib} ^d

Coordination of 1-isopropyl-3,5-dipyridyl-6-oxoverdazyl to cobalt results in a dication best described in the solid state as a high spin cobalt(II) ion coordinated to two radical ligands with an $S = 3/2$ ground state. On dissolution in acetonitrile, the cobalt(II) form equilibrates with a cobalt(III) valence tautomer with an $S = 1/2$ ground state.

Valence tautomerization is a form of isomerism involving the redistribution of electrons between isomeric forms. In inorganic chemistry it typically involves the distribution of electrons between a metal center and redox active ligand.^{1,2} Valence tautomers often differ in their spin multiplicity and geometry and have potential application as molecular switches or other molecular devices,^{3–6} and on the macroscopic scale can result in remarkable properties such as photomechanical effects.^{7,8} The majority of known inorganic valence tautomers involve oxolene (catechol/semiquinone/quinone) ligands or related iminoquinones. Though other ligand examples are known they are few and far between.² Consequently, finding new examples of valence tautomeric systems is important for further development of the area, not only by improving basic understanding of the phenomenon, but also by providing a greater diversity of coordination environments and geometries suitable for practical applications. Verdazyl radicals have significant potential in this area. Verdazyl coordination chemistry has been studied for the past twenty years and has

revealed remarkably strong magnetic exchange interactions between the radicals and coordinated metal ions.⁹ Verdazyl coordination compounds are analogous to polypyridine systems, resulting in predictable coordination geometry and the potential for self-assembly to form complex, programmed structures.^{10–12} Furthermore, verdazyls are redox active and maintain this activity when coordinated to metal ions,^{13–15} as well as showing more complex behavior. In some early examples electron density on the verdazyl ring was shown to be sensitive to ancillary ligands on the metal resulting in a shift from anion-like to radical-like ligand behavior.^{16,17} More recently, we reported an iron verdazyl complex for which the electron delocalization over both verdazyl ligands resulted in remarkably strong ferromagnetic exchange.¹⁸ To search for further examples of electronically labile compounds supported by verdazyl ligands, cobalt compounds are attractive targets. Cobalt oxolene compounds were some of the first reported valence tautomers, while cobalt bis-terpyridine, and various related structures, show temperature-dependent spin crossover.^{19–21} Here we report an example of valence tautomerization and an unusual electronic structure in a cobalt verdazyl complex, illustrating the strong metal–ligand interaction characteristic of these systems.

The tridentate dipyrldyl verdazyl ligand (dipyvdl) was initially reported in the synthesis of a nickel complex which was synthesized through the direct reaction of metal with the ligand.²² More recently we have reported that synthesis of metal complexes from the corresponding leucoverdazyl is more reproducible.¹⁸ Combination of the leucoverdazyl with cobalt(II) triflate in acetonitrile gave a transient green-brown solution that was rapidly oxidized in air to give a deep green species crystallized as the hexafluorophosphate salt (Scheme 1).

Electrospray MS gave a molecular ion with $m/z = 649$, consistent with a 2:1 ligand to metal stoichiometry. The diamagnetism of this compound, with sharp ¹H and ¹³C NMR spectra (ESI†) consistent with only one ligand environment, indicate the compound is best described as a low-spin cobalt(III) complex with two diamagnetic, anionic ligands. Prior studies have shown a dependence of the oxoverdazyl C=O bond stretch on the oxidation state of the ligand; reduced ligands

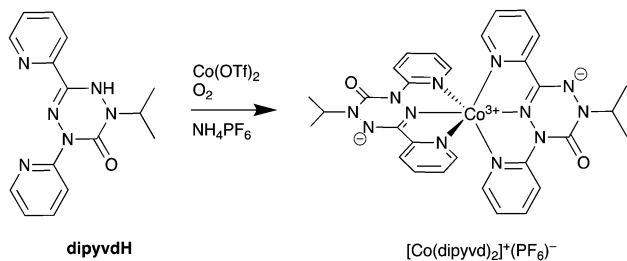
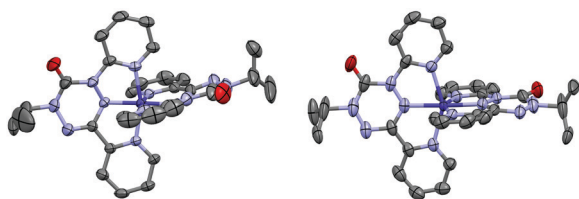
^a Department of Chemistry, San Jose State University, One Washington Square, San Jose, CA 95126, USA. E-mail: david.brook@sjsu.edu

^b Department of Physics, University of South Florida, Tampa, Florida 33620, USA

^c National High Magnetic Field Laboratory, Florida State University, 1800 E. Paul Dirac Drive, Tallahassee, FL 32310, USA

^d Department of Chemistry, University of Idaho, 875 Perimeter Drive, Moscow, ID 83844, USA

† Electronic supplementary information (ESI) available: Details of the synthesis of [Co(dipyvdl)₂](PF₆)₂ and [Co(dipyvdl)₂](PF₆)₂, ¹H and ¹³C NMR spectra of [Co(dipyvdl)₂](PF₆)₂, high field EPR spectra of [Co(dipyvdl)₂](PF₆)₂, calculated and observed X-ray diffraction patterns of [Co(dipyvdl)₂](PF₆)₂, cyclic voltammogram for the [Co(dipyvdl)₂]²⁺ system in acetonitrile, fit of the low temperature magnetic susceptibility data for [Co(dipyvdl)₂](PF₆)₂. Full details of the crystal structures of [Co(dipyvdl)₂](PF₆)₂ and [Co(dipyvdl)₂](PF₆)₂. CCDC 1885262 and 1885263. For ESI and crystallographic data in CIF or other electronic format see DOI: 10.1039/d0cc01770a

Scheme 1 Synthesis of $[\text{Co}(\text{dipyvd})_2](\text{PF}_6)_2$.Fig. 1 Thermal ellipsoid plots of the cation in $[\text{Co}(\text{dipyvd})_2]^{2+}(\text{PF}_6^-)_2$ (left) and $[\text{Co}(\text{dipyvd})_2]^{2+}(\text{PF}_6^-)_2$ (right). Ellipsoids are drawn at the 50% level. Hydrogen atoms have been omitted for clarity.

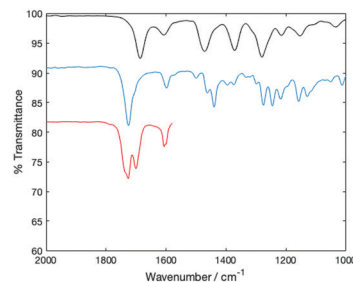
giving a lower vibrational frequency.¹⁶ Consistent with the verdazyl anion formulation, the C=O stretch at 1685 cm^{-1} is lower than that of the coordinated radical in $[\text{Ni}(\text{dipyvd})_2]^{2+}$ (at 1725 cm^{-1})²² or even the partly reduced ligand system in $[\text{Fe}(\text{dipyvd})_2]^+$ (1690 cm^{-1}).¹⁸ Single crystals were grown from dichloromethane/octane and studied by X-ray diffraction. A thermal ellipsoid plot is shown in Fig. 1 and select bond lengths are listed in Table 1. Notably the short metal ligand bond lengths and non-planar tetrazine rings are consistent with the cobalt(III)/anionic ligand formulation.

Cyclic voltammetry in acetonitrile indicates that this species undergoes a single one electron reduction at -0.20 V vs. SCE and two successive one electron oxidations at $+0.58\text{ V}$ and $+0.95\text{ V}$ vs. SCE (ESI[†]). Based on this electrochemical data, the dication $[\text{Co}(\text{dipyvd})_2]^{2+}$ was generated through oxidation with one equivalent of AgPF_6 in dichloromethane to give a dark green precipitate. The IR spectrum of this material was almost identical to that for the previously characterized Ni^{2+} complex, featuring a prominent ligand C=O stretch at 1725 cm^{-1} (Fig. 2).

Table 1 Selected crystallographic bond lengths for $[\text{Co}(\text{dipyvd})_2]^{2+}(\text{PF}_6^-)_2$ and $[\text{Co}(\text{dipyvd})_2]^{2+}(\text{PF}_6^-)_2$

Bond	$[\text{Co}(\text{dipyvd})_2]^{2+}(\text{PF}_6^-)_2^a$	$[\text{Co}(\text{dipyvd})_2]^{2+}(\text{PF}_6^-)_2$
M-N1	1.872	2.006
M-N5	1.926	2.138 ^b
M-N6	1.945	2.139 ^b
N3-N4	1.390	1.336 ^b
N1-N2	1.427	1.353 ^b
Planarity ^c	0.12	0.03

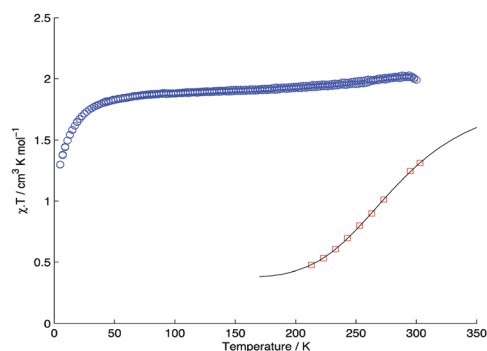
^a Bonds associated with one of two crystallographically independent ligands. The second ligand showed similar geometry but was disordered over two possible orientations. ^b Average bond lengths as a result of orientational disorder. ^c Planarity of the verdazyl ring was measured as the mean distance of the ring atoms from the mean plane defined by those atoms.

Fig. 2 Infrared spectra of $[\text{Co}(\text{dipyvd})_2](\text{PF}_6)_2$ (black), solid $[\text{Co}(\text{dipyvd})_2](\text{PF}_6)_2$ (blue) and $[\text{Co}(\text{dipyvd})_2](\text{PF}_6)_2$ in acetonitrile solution (red).

X-ray powder diffraction (ESI[†]) indicated the material contained metallic silver, along with a phase with a tetragonal unit cell with dimensions $a = 15.84\text{ \AA}$, $c = 15.37\text{ \AA}$, isomorphous with the previously reported nickel²² and iron species.¹⁸

Elemental analysis and mass spectrometry were consistent with the conservation of the 2 : 1 ligand : metal ratio, along with co-precipitation of approximately one equivalent of metallic silver as would be expected from the reaction stoichiometry. The material was paramagnetic with $\chi T = 1.92$ at room temperature; χT was only weakly temperature dependent above 50 K; below this temperature it dropped more sharply to 1.3 at 5 K (Fig. 3). Metallic silver was removed by dissolution in acetone and filtration, followed by diffusion of ether into the solution to induce crystallization. A single crystal was isolated that matched the previously determined tetragonal unit cell; full analysis by X-ray diffraction confirmed the previously noted isomorphism and gave metal-ligand bond lengths consistent with a high spin metal ion (Table 1).

The high-frequency (HF) EPR spectra recorded at 5 K for neat powder samples of $[\text{Co}(\text{dipyvd})_2](\text{PF}_6)_2$ exhibit two resonances which, based on their field vs. frequency dependence, have an effective g value of 4.5 and 2.0 respectively (Fig. 4 and ESI[†]). Such spectra are characteristic of a quasi-axial, positive zero-field splitting (ZFS). Therefore, they originate from the $|S, m\rangle = |3/2, \pm 1/2\rangle$ round Kramers doublet of a $S = 3/2$ system with $D > 0$ and vanishing E/D value. The linewidth of the low-field transition increases with frequency suggesting that g_x and g_y are not equal; unfortunately, they are unresolved. The excited

Fig. 3 Plot of χT vs. T for crystalline $[\text{Co}(\text{dipyvd})_2]^{2+}(\text{PF}_6)_2$ (blue circles) and $[\text{Co}(\text{dipyvd})_2]^{2+}(\text{PF}_6)_2$ in acetonitrile solution (red squares). The solid line corresponds to the equilibrium model described in the text (with $g = 2$, $H = 18.7\text{ kJ mol}^{-1}$, $S = 66\text{ J mol}^{-1}\text{ K}^{-1}$).

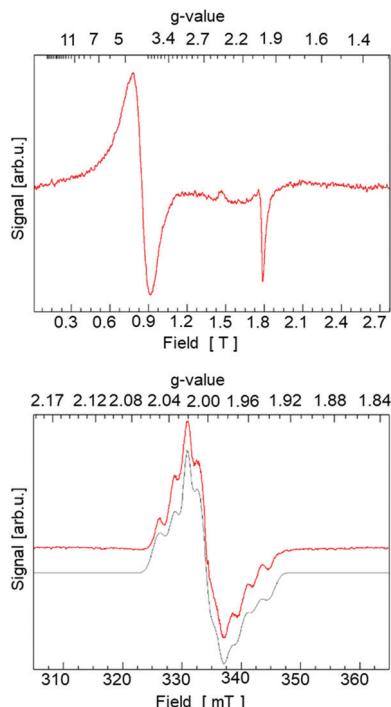


Fig. 4 CW EPR spectra recorded for $[\text{Co}(\text{dipyvd})_2]^{2+}(\text{PF}_6)_2$. Top: Spectrum recorded at 5 K and 50.3 GHz for a neat powder sample of $[\text{Co}(\text{dipyvd})_2]^{2+}(\text{PF}_6)_2$. Bottom: X-band EPR spectrum recorded at 77 K for a MeCN solution of $[\text{Co}(\text{dipyvd})_2]^{2+}(\text{PF}_6)_2$. The experimental spectrum shown in red was recorded using a microwave frequency of 9.36 GHz, modulation amplitude of 3 G, modulation frequency of 100 kHz, and microwave power of 2 mW. Shown in black is a simulation obtained for a $S = 1/2$ and $I = 7/2$ such that $g_x = 1.988$, $g_y = 1.994$, $g_z = 2.011$, $\sigma(g_x) = 0.009$, $\sigma(g_y) = 0.005$, $\sigma(g_z) = 0.001$, $A_x = 8.42$ MHz, $A_y = 75$ MHz, $A_z = 10.46$ MHz, and an intrinsic linewidth of 6 G.

Kramers doublet of such species is expected to be EPR silent. Furthermore, no inter-Kramers transitions were observed even for frequencies as high as 400 GHz. The magnitude of the ZFS was estimated from the least-square fitting of the low temperature χT data (ESI[†]) which suggested that $D = 16(2)$ cm^{-1} and $E/D = 0.05(5)$. The large magnitude ZFS tensor is further corroborated by the linear dependence of field vs. frequency of the observed resonances (ESI[†]).

Unlike for the solid, the solution magnetic susceptibility, determined using Evans' NMR method, shows a strong temperature dependence (Fig. 3) and solutions in acetonitrile show an additional IR C=O stretch at 1700 cm^{-1} (Fig. 2). Although the initial precipitate was EPR-silent at 77 K, frozen acetonitrile solutions investigated at 77 K showed a signal centered at $g = 2$ with a rich hyperfine structure, (Fig. 4). In stark contrast to the spectra recorded for neat powder samples, this spectrum demonstrates the presence, for frozen solutions, of a $S = 1/2$ signal. Analysis of the hyperfine splitting pattern originating from the interaction of the electronic spin with the $I = 7/2$ of ^{59}Co (100%) nuclei reveals a practically quenched hyperfine coupling tensor. Together with the nearly isotropic g -tensor for which $g_{\text{iso}} = 1.998$ ($\cong g_e$) this observation indicates that the unpaired electron is localized on the ligand and that the cobalt ion is diamagnetic consistent with the presence of a low-spin $\text{Co}(\text{III})$ metal center.

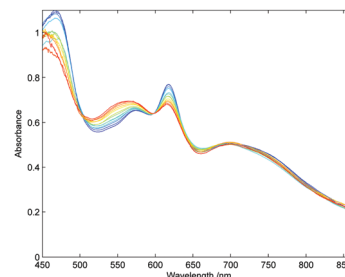


Fig. 5 Visible spectra of $[\text{Co}(\text{dipyvd})_2]^{2+}$ in acetonitrile solution from $-6\text{ }^\circ\text{C}$ (blue) to $38\text{ }^\circ\text{C}$ (red).

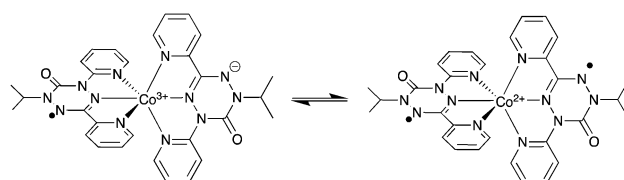
The UV-vis also shows a distinct temperature dependence (Fig. 5) consistent with an equilibrium between two species. Taken together these observations are consistent with a valence tautomeric equilibrium in solution between an $S = 3/2$ cobalt(II)/diradical species and an $S = 1/2$ cobalt(III)/radical/anion species (Scheme 2).

Considering that the low-temperature solution susceptibility approaches the spin-only value for an $S = 1/2$ system, we assumed an equilibrium between an $S = 1/2$ and an $S = 3/2$ system and used the values to determine the associated enthalpy and entropy obtaining $\Delta H = 18.7(1)$ kJ mol^{-1} and $\Delta S = 66.0(3)$ $\text{J mol}^{-1} \text{K}^{-1}$ (Fig. 3).

Though non-innocent behavior has been noted before in verdazyl coordination systems, the valence tautomerism reported here is unique. Hicks has reported a change in electronic distribution in ruthenium verdazyl systems resulting from a change in ancillary ligand,^{16,17} but no equilibrium between verdazyl valence tautomers has been reported until now.

The switch between the two tautomers in solution and the presence of different forms at low temperature in solution vs. solid indicates that the equilibrium can be strongly influenced by changes in molecular environment. In addition to temperature-induced changes in solution, this could provide a path to control the switching between tautomers in the solid state. The latter has particular significance for this ligand because of its structural relationship to polytopic terpyridyl based ligands capable of self-assembly.

The apparent high-spin $\text{Co}(\text{II})$ state observed for the tetragonal form of $[\text{Co}(\text{dipyvd})_2]^{2+}$ is unusual. The magnetic data and HF EPR spectra collected for neat powder samples demonstrate, unambiguously, a $S = 3/2$ ground state in solid state. Although a quartet can be obtained from the ferromagnetic coupling of two $S = 1/2$ radical spins with a low-spin $\text{Co}(\text{II})$ ion, the large positive ZFS of this quartet, $D = 16(2)$ cm^{-1} , indicate that in the solid state $[\text{Co}(\text{dipyvd})_2](\text{PF}_6)_2$ incorporates a high-spin $\text{Co}(\text{II})$ ion.



Scheme 2 Valence tautomeric equilibrium in $[\text{Co}(\text{dipyvd})_2]^{2+}$.

This conclusion is further validated by the low-temperature crystallographic studies of this complex which revealed a geometry consistent with high spin Co^{2+} coordinated to two radical ligands. However, the direct exchange interactions between the metal ion and ligand-based spins are expected to be strongly antiferromagnetic and to lead to an overall $S = 1/2$ system. Instead, the observation of an $S = 3/2$ system is puzzling and is indicative for the presence of either dissimilar ligands such that one is ferromagnetically and the other is antiferromagnetically coupled to the metal spin or to a strong antiferromagnetic interaction between the ligand spins consistent with the presence of spin frustration. The situation is all the more puzzling since the only other reported cobalt-verdazyl systems report relatively strong ferromagnetic coupling.^{23,24}

A similar intermediate spin state has been observed in a cobalt pyridyl-diimine (PDI) system: Bowman and co-workers reported an $S = 3/2$ ground state for the neutral complex $\text{Co}(\text{PDI})_2$ which has a high spin Co^{2+} ion, and two nominally radical-anionic ligands.²⁵ Their explanation considered antiferromagnetic exchange between one of the ligand SOMOs and the remaining half occupied t_{2g} orbital, leaving the other ligand SOMO to couple ferromagnetically with the e_g (d_{σ}) orbital set. While qualitatively providing the correct answer, the authors mention that this model is probably overly simplistic, especially since there is no other evidence of a difference between the two ligands. Several cobalt bis(semiquinones) systems also feature a high spin Co^{2+} ion and an overall $S = 3/2$ spin, either as the ground state²⁶ or more typically as an excited valence tautomer.²⁷ A coherent explanation of these states is similarly elusive, though the difference in coordination geometry makes comparison with the current system more tenuous. Nevertheless, our observation of the $S = 3/2$ state in $[\text{Co}(\text{dipyvd})_2]^{2+}$ emphasizes that the cobalt dioxolene systems are not an isolated oddity and that there is still more to be learned about magnetic exchange interactions even in apparently straightforward situations.

In summary, we have discovered a new valence tautomeric system involving cobalt and a polypyridyl type ligand. Not only does this system differ from the more typical semiquinone-catecholate valence tautomers, it is also unique in that the valence tautomeric equilibrium is only observed in solution, while the solid state effectively traps the molecule in the high spin state. This illustrates the delicate balance of interactions that result in valence tautomerization, and also provides a unique opportunity to manipulate the equilibrium between tautomers by, for example, changing the counterions in the solid state. An understanding of the intermolecular forces that control the equilibrium combined with the predictable coordination geometry provided by the polypyridyl-type structure should provide further opportunities for molecular switches and more complex functional systems driven by valence tautomerism.

Financial support was provided by the National Science Foundation Grants CHE-1058077 and CHE-1900491 (to DJRB) and the NIH-MBRS RISE program (5R25GEMO71381). A portion

of this work was performed at the National High Magnetic Field Laboratory, which is supported by National Science Foundation Cooperative Agreement No. DMR-1644779 and the State of Florida. Crystallographic data were collected through the SCrALS program at the Advanced Light Source (ALS). The ALS is supported by the U.S. Department of Energy, Office of Energy Sciences Materials Sciences Division, under contract DE-AC02-05CH11231 at Lawrence Berkeley National Laboratory. SAS acknowledges support from the University of Idaho.

Conflicts of interest

There are no conflicts to declare.

Notes and references

- 1 A. B. Gaspar and M. Sereydyuk, *Coord. Chem. Rev.*, 2014, **268**, 41–58.
- 2 T. Tezgerevska, K. G. Alley and C. Boskovic, *Coord. Chem. Rev.*, 2014, **268**, 23–40.
- 3 J. Ferrando-Soria, J. Vallejo, M. Castellano, J. Martinez-Lillo, E. Pardo, J. Cano, I. Castro, F. Lloret, R. Ruiz-García and M. Julve, *Coord. Chem. Rev.*, 2017, **339**, 17–103.
- 4 A. A. Starikova and V. I. Minkin, *New J. Chem.*, 2017, **41**, 6497–6503.
- 5 A. Lannes, Y. Suffren, J. B. Tommasino, R. Chiriac, F. Toche, L. Khrouz, F. Molton, C. Duboc, I. Kieffer, J.-L. Hazemann, C. Reber, A. Hauser and D. Luneau, *J. Am. Chem. Soc.*, 2016, **138**, 16493–16501.
- 6 N. A. Vazquez-Mera, F. Novio, C. Roscini, C. Bellacanzone, M. Guardingo, J. Hernando and D. Ruiz-Molina, *J. Mater. Chem. C*, 2016, **4**, 5879–5889.
- 7 O. S. Jung and C. G. Pierpont, *J. Am. Chem. Soc.*, 1994, **116**, 2229–2230.
- 8 C. W. Lange, M. Foldeaki, V. I. Nevodchikov, V. K. Cherkasov, G. A. Abakumov and C. G. Pierpont, *J. Am. Chem. Soc.*, 1992, **114**, 4220–4222.
- 9 D. J. R. Brook, *Comments Inorg. Chem.*, 2015, **35**, 1–17.
- 10 M. Barboiu and J. M. Lehn, *Rev. Roum. Chim.*, 2006, **51**, 581–588.
- 11 G. S. Hanan, C. R. Arana, J.-M. Lehn, G. Baum and D. Fenske, *Chem. – Eur. J.*, 1996, **2**, 1292–1302.
- 12 J. M. Lehn, *Supramolecular Chemistry*, VCH, Weinheim, 1995.
- 13 K. J. Anderson, J. B. Gilroy, B. O. Patrick, R. McDonald, M. J. Ferguson and R. G. Hicks, *Inorg. Chim. Acta*, 2011, **374**, 480–488.
- 14 J. B. Gilroy, S. D. J. McKinnon, B. D. Koivisto and R. G. Hicks, *Org. Lett.*, 2007, **9**, 4837–4840.
- 15 C. A. Sanz, M. J. Ferguson, R. McDonald, B. O. Patrick and R. G. Hicks, *Chem. Commun.*, 2014, **50**, 11676–11678.
- 16 S. D. J. McKinnon, B. O. Patrick, A. B. P. Lever and R. G. Hicks, *Chem. Commun.*, 2010, **46**, 773–775.
- 17 S. D. J. McKinnon, B. O. Patrick, A. B. P. Lever and R. G. Hicks, *Inorg. Chem.*, 2013, **52**, 8053–8066.
- 18 D. J. R. Brook, C. Fleming, D. Chung, C. Richardson, S. Ponce, R. Das, H. Srikanth, R. Heindl and B. C. Noll, *Dalton Trans.*, 2018, **47**, 6351–6360.
- 19 J. S. Judge and W. A. J. Baker, *Inorg. Chim. Acta*, 1967, **1**, 68.
- 20 S. Kremer, W. Henke and D. Reinen, *Inorg. Chem.*, 1982, **21**, 3013–3022.
- 21 P. Nielsen, H. Toftlund, A. D. Bond, J. F. Boas, J. R. Pilbrow, G. R. Hanson, C. Noble, M. J. Riley, S. M. Neville, B. Moubaraki and K. S. Murray, *Inorg. Chem.*, 2009, **48**, 7033–7047.
- 22 C. Richardson, B. Haller, D. J. R. Brook, M. Hundley and G. T. Yee, *Chem. Commun.*, 2010, **46**, 6590–6592.
- 23 T. M. Barclay, R. G. Hicks, M. T. Lemaire, L. K. Thompson and Z. Q. Xu, *Chem. Commun.*, 2002, 1688–1689.
- 24 M. T. Lemaire, T. M. Barclay, L. K. Thompson and R. G. Hicks, *Inorg. Chim. Acta*, 2006, **359**, 2616–2621.
- 25 A. C. Bowman, C. Milsman, E. Bill, E. Lobkovsky, T. Weyhermüller, K. Wieghardt and P. J. Chirik, *Inorg. Chem.*, 2010, **49**, 6110–6123.
- 26 N. A. Protasenko, A. I. Poddel'sky, A. S. Bogomyakov, N. V. Somov, G. A. Abakumov and V. K. Cherkasov, *Polyhedron*, 2013, **49**, 239–243.
- 27 H. W. Liang, T. Kroll, D. Nordlund, T.-C. Weng, D. Sokaras, C. G. Pierpont and K. J. Gaffney, *Inorg. Chem.*, 2017, **56**, 737–747.